Electronic Spectrum of Anthracene: An ab-Initio Molecular Orbital Calculation Combined with a Valence Bond Interpretation

Shmuel Zilberg,[†] Yehuda Haas,*,[†] and Sason Shaik[‡]

Department of Physical Chemistry, the Farkas Center for Light Induced Processes, and the Department of Organic Chemistry, The Hebrew University of Jerusalem, Jerusalem, Israel

Received: June 5, 1995; In Final Form: August 28, 1995[⊗]

The properties of the two lowest excited singlet states of anthracene, $S_1(^1B_{1u})$ and $S_2(^1B_{2u})$, and the first triplet state, $T_1(^3B_{1u})$, were calculated at the CIS/3-21G level of theory. The main structural changes are described, and the calculated vibrational levels are compared with available experimental data. The assignment of the two-photon observed transition at about 28 000 cm^{-1} to the S_2 state is confirmed, as well as some recent argon matrix vibronic bands (Wolf, J.; Hohlneicher, G. *Chem. Phys.* **1994**, *181*, 185). The calculation suggests some changes in the vibrational assignment, and correlation with the ground state vibrational modes shows that one b_{2u} mode undergoes a large frequency increase upon electronic excitation to S_2. This change is similar to that observed for Kekulé-type modes of benzene, naphthalene, and their derivatives. It is compatible with the notion that the π electrons of these molecules tend to distort the molecule to a Kekulé structure.

I. Introduction

Several recent papers have dealt with the electronic spectrum of anthracene,[1,2] mainly in an attempt to assign the vibronic structure, which in turn is the key to the understanding of the photodynamics of the molecule. It is well-known that the two lowest lying singlet states ($^1B_{1u}$ and $^1B_{2u}$, ^1L_a and ^1L_b in Platt's notation[3]) are very close in energy.[4] One-photon transitions from the ground state to the latter, which is the lowest lying excited state in benzene and naphthalene, are symmetry forbidden. Nonetheless, although the oscillator strength for transition from the ground state is 2−3 orders of magnitude smaller than that leading to the L_a state, the transition is clearly observed in benzene and naphthalene (and in their derivatives). In anthracene, the order is reversed, and the $1^1A_g \rightarrow 1^1B_{2u}$ band is hidden under the much stronger $1^1A_g \rightarrow 1^1B_{1u}$ one. In two-photon absorption spectroscopy, the transition to the 1^1B_{2u} state is more easily observed because it is expected to have a higher intensity than the transition to the 1^1B_{1u} one.[5] The $g \nleftrightarrow g$ selection rule for two-photon transitions forbids the direct observation of the origin of both of these transitions, so that experimental determination of the zero-point energy of the 1^1B_{2u} state remains a challenge. Wolf and Hohlneicher (WH) have recently summarized the available information and reported an extensive two-photon fluorescence excitation study of anthracene in an argon matrix.[1] Several vibronic bands, mostly of b_{2u} symmetry, were recorded and ascribed to the 1^1B_{2u} state, allowing an approximate determination of its origin.

Some b_{2u} vibrational modes are referred to as "Kekulé-type" modes, since they involve carbon atom displacements that distort the molecule to a Kekulé structure. It has been noticed that the $\nu_{14}(b_{2u})$ mode of benzene and the $\nu_{21}(b_{2u})$ mode of naphthalene—both Kekulé-type—undergo a considerable frequency increase upon excitation of the molecules from the S_0-(^1A_g) to the $S_1(^1B_{2u})$ state.[6−8] This increase has been recently interpreted[9] to indicate that the D_{6h} symmetry of benzene is determined by the six-membered-ring σ-bond structure, while π electrons tend to distort the molecule to a D_{3h} symmetry, i.e. to a Kekulé structure, as predicted by the avoided crossing model of Shaik and Hiberty.[10] Excitation of an electron from a π-bonding orbital to an antibonding π^* one decreases the distortive tendency and leads to a larger restoring force (and frequency) of the vibrational mode corresponding to this b_{2u} coordinate.

According to WH's analysis, the most intense band in the $1^1A_g \rightarrow 1^1B_{2u}$ spectrum of anthracene appears at a frequency of 1548 cm^{-1}, a value close to that reported for the Kekulé-type vibrations of benzene (1570 cm^{-1})[6,7] and naphthalene (1548 cm^{-1})[8] in their respective 1^1B_{2u} states. A still higher frequency band, at 1695 cm^{-1}, was tentatively assigned also to a skeletal b_{2u} vibrational mode. This relatively high value for such a vibration was one of the reasons for the present undertaking, a theoretical calculation of the vibrational modes of the excited state. Furthermore, the interpretation cited for benzene and naphthalene should also hold for anthracene, in which case the 1548 cm^{-1} mode of the 1^1B_{2u} state should correlate with the 1318 cm^{-1} ($6b_{2u}$) mode observed by infrared spectroscopy[11] and not with the higher frequency 1460 ($4b_{2u}$) or 1541 ($3b_{2u}$) cm^{-1} ones.

The assignment of the vibronic structure of the absorption spectra requires the knowledge of the force fields of electronically excited states. These are often not readily available, and the ground state force constants were used frequently to guide the assignment. Molecular orbital (MO) ab-initio calculations are being increasingly used for this purpose for polyatomic molecules of intermediate size (10−30 atoms).[12−14] The availability of powerful and relatively cheap workstations and of commercial ab-initio programs makes it possible to test several approaches for the solution of the vibronic analysis problem, at various levels of theory. Recently, we have published an ab-initio calculation of the S_0, S_1, and T_1 states of anthracene,[2] along with their normal modes, using the UHF method[15] to calculate the properties of the excited states. The present work reports an extension of that study, in which the excited states are calculated at a higher level, using the configuration interaction singles (CIS) method.[16] As shall be seen, the results support in general the assignment of the 1^1B_{2u}

[†] Department of Physical Chemistry and the Farkas Center for Light Induced Processes.
[‡] Department of Organic Chemistry.
[⊗] Abstract published in *Advance ACS Abstracts*, October 15, 1995.

0022-3654/95/2099-16558$09.00/0

TABLE 1: Calculated (CIS/3-21G) and Experimental Properties of Anthracene in Some Electronic States

	S_0		S_1		S_2		T_1	
	exp	calc	exp	calc	exp	calc	exp	calc
energy (eV)	0	0	3.43[a] 3.37[b]	4.29	3.47[b]	4.91	1.85[c]	1.65
rotational constants (MHz)								
A	2151[d]	2183.0	2159[d]	2198.6		2140.3		2202.7
ΔA[e]			8	15.6				
B	453.8[d]	458.0	444.5[d]	451.6		454.9		449.5
ΔB[e]			−9.3	−6.4				
C	374.7[d]	378.6	368.3[d]	374.7		375.1		373.3
ΔC[e]			−6.4	−3.9				
oscillator strength ($S_0 \rightarrow S_1$)			0.1[f]	0.23		0.0006		0

[a] In the gas phase.[39] [b] In an argon matrix.[1] [c] In an *n*-heptane matrix.[40] [d] Reference 24. [e] The change in the rotational constant upon excitation from S_0 to S_1. [f] Reference 20.

state's vibronic structure given in ref 1 (with some modifications) and show that the Kekulé-type vibration does indeed undergo the expected upward shift upon excitation of the molecule to this state.

While the frequency increase of the Kekulé-type b_{2u} mode in the 1^1B_{2u} state in anthracene is calculated in this paper using the MO theory, physical insight into the origin of this frequency exaltation is more readily available by the valence bond (VB) approach.[17] An extensive VB calculation of benzene[18] shows that the ground ($S_0(1^1A_g)$) and the $S_1(1^1B_{2u})$ states are essentially covalent in nature, and straightforward symmetry arguments show that the main contribution to the total wave functions of these states comes from an in-phase and out-of-phase combination of the two Kekulé-type VB wave functions, respectively. We propose an analogous explanation also for other aromatic molecules, and in this paper we discuss the case of anthracene, for which four independent Kekulé structures can be written.

II. Computational Details

Calculations were performed using the Gaussian 92 program package,[19] on a Silicon Graphics Indigo R4000/48MB/2GBHD workstation. The ground state (S_0) calculations were performed at the HF/3-21G level of theory, while S_1, S_2, and T_1 were studied by the configuration interaction singles (CIS) procedure,[16] using the same basis set.[21] Full geometrical optimization was performed for each state, and the optimum geometry was ascertained by vibrational frequency calculations (no imaginary values). The vibrational frequencies, at the harmonic approximation, were obtained by computing the Hessian matrix. The required second derivatives of the potential were calculated analytically for S_0 and numerically for the excited states. All frequencies quoted below were obtained from the computed ones by multiplying with appropriate scaling factors.[22] The same factors (0.89 for the in-plane and 0.85 for the out-of-plane modes) were used for all electronic states. In some cases the CIS energies were further corrected by applying second-order Moller–Plesset perturbation treatment; the values so obtained are referred to as CIS-MP2 energies.

III. Results

III.a. Energy and Structure of the Excited States. The CIS method involves all configurations which arise from a single-electron excitation of the HF determinant of the ground state. Scheme 1 shows a schematic representation of the two highest occupied MOs and of the two lowest unoccupied ones. It was found that the main contribution to the first electronically excited state, S_1, comes from the configuration $\{...(b_{1g})^2(b_{2g})^1(b_{3u})^1\}$ arising from HOMO(b_{2g}) → LUMO(b_{3u}) excitation and resulting in a $^1B_{1u}$ state. The next largest contribution, due to

SCHEME 1: Schematic Representation of the Two HOMOs and the Two LUMOs and the Electronic Configurations of the 1^1A_g, 1^1B_{1u}, and 1^1B_{2u} States of Anthracene

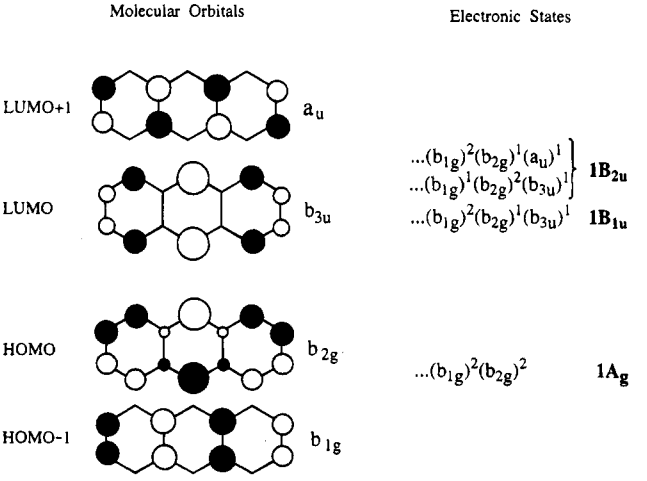

the HOMO−1(b_{1g}) → LUMO+1(a_u) excitation, has a coefficient which is 9 times smaller than that of the leading term. In contrast, the S_2 state arises from essentially equal contributions of the HOMO(b_{2g}) → LUMO+1(a_u) and the HOMO−1(b_{1g}) → LUMO(b_{3u}) configurations, both leading to a $^1B_{2u}$ state. This latter state is the lowest energy one in benzene and naphthalene, but the 1^1B_{1u}–1^1B_{2u} order is reversed in anthracene and larger acenes.[23]

The calculated energies, dipole moments, and rotational constants of the three excited states are listed in Table 1, along with the data calculated for the ground state. The oscillator strengths for transitions from the ground state to the excited states are also shown. The molecule is found to retain its planar form in the three states, and Figure 1 shows the changes in the C–C bond lengths. For a given symmetry, changes with respect to the ground state are similar for the singlet and triplet states. In the B_{1u} states, the middle ring expands a little, and the outer ones become more symmetric, their five edges calculated to be of almost equal length. In $S_2(1^1B_{2u})$ the "inner" CC bond lengths (C11–C12 and C13–C14) are considerably elongated (to 1.480 Å) by comparison with the lower states. The experimental rotational constants are derived[24] from X-ray diffraction data for the ground state and from purely rotational coherence spectroscopy for S_1. The precision of both methods is such that the small changes taking place upon electronic excitation are subject to a large error. It has been estimated that the decrease in the B and C constants is real and represents a ~1% stretch of the molecule in the direction of its long axis. This trend is reproduced by the calculation. The change in the

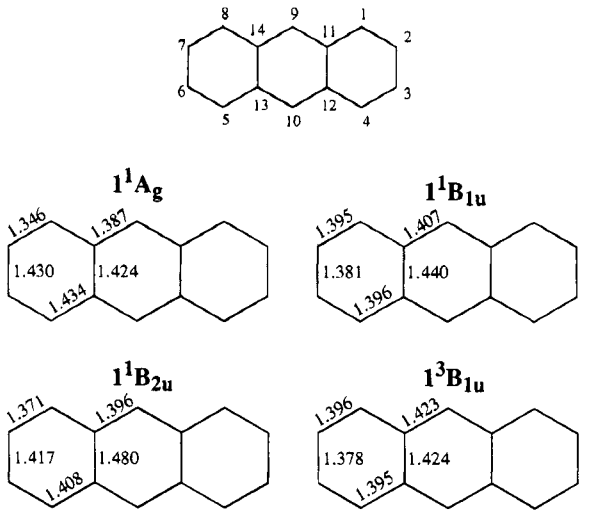

Figure 1. Calculated C−C bond lengths in the different electronic states. The atom numbering convention is also shown.

TABLE 2: Calculated and Experimental Geometry of Anthracene in Some Electronically Excited States[a]

	HF/3-21G ground state[c]	CIS/3-21G $T_1(1^3B_{2u})$	CIS/3-21G $S_1(1^1B_{1u})$	CIS/3-21G $S_2(1^1B_{2u})$
		Bonds[b]		
C_9C_{11} (a)	1.387 (1.392)	1.423	1.407	1.396
Δa		+0.036	+.0020	+.009
C_1C_{11} (b)	1.434 (1.437)	1.395	1.396	1.408
Δb		−.039	−.038	−.026
C_1C_2 (c)	1.346 (1.397)	1.396	1.395	1.371
Δc		+.050	+.049	+.025
C_2C_3 (d)	1.430 (1.422)	1.378	1.381	1.417
Δd		−.052	−.049	−.013
$C_{11}C_{12}$ (e)	1.424 (1.437)	1.424	1.440	1.480
Δe		.000	+.016	+.056
C_9H_9	1.047	1.073	1.074	1.074
C_1H_1	1.073	1.072	1.073	1.073
C_2H_2	1.072	1.072	1.071	1.071
		Angles[d]		
$C_{11}C_9C_{14}$	121.5 (121.0)	122.1	122.8	122.4
$C_9C_{11}C_{12}$	119.3 (118.43)	118.3	118.6	118.8
$C_1C_{11}C_{12}$	119.3 (119.30)	119.0	118.7	118.1
$C_2C_1C_{11}$	120.9 (120.34)	121.0	121.3	121.4
$C_1C_2C_3$	120.1 (120.43)	120.0	120.1	120.5
$H_1C_1C_2$	120.8	119.8	119.7	120.1
$H_1C_1C_{11}$	118.3	119.2	119.1	118.5
$H_2C_2C_1$	120.5	119.2	119.1	118.5
$H_2C_2C_3$	119.0	120.3	120.4	119.5
$H_9C_9C_{11}$	119.3	118.9	118.3	118.8

[a] Distances in angstrom units. [b] See Figure 1 for notation; Δx is the difference between the calculated length of bond x in the excited and ground states. [c] In parentheses: experimental values from the electron diffraction study in the following: Ketkar, S. N.; Kelley, M.; Fink, M.; Ivey, R. C. *J. Mol. Struct.* **1981**, *77*, 127. [d] Angles in degrees.

direction of the short axis has been claimed to be indeterminate; the calculation predicts a very small elongation in that direction. Table 2 and Figure 1 give a complete summary of the calculated bond length changes and compares the ground state values with experimental ones.

III.b. Vibrational Frequencies. Table 3 lists the calculated frequencies for the four electronic states and compares them with available experimental data. One-photon spectroscopic results, obtained in the gas and condensed phase, were discussed extensively in our recent communications[2,25] and by Hohlneicher's group.[1,14] The $S_0 \rightarrow S_2$ transition was extensively studied in several condensed phase environments; the recent argon matrix data of ref 1 are shown in the Table 3. For consistency, one-photon results obtained in an argon matrix are also used; it has been shown that they are usually close to the gas phase values (see Table 5 of ref 2).

III.b.1. The Singlet $^1B_{1u}$ and $^1B_{2u}$ States. The vibrational analysis of the one-photon spectrum of the $S_0 \rightarrow S_1$ transition, based on a UHF/3-21G calculation, was given in the previous paper.[2] Comparison of the calculations presented in this paper with the previous ones reveals only minor changes and does not lead to any change in the proposed assignments. The b_{1u} and b_{2u} modes are not one-photon active and were not discussed; here we compare our present calculations for the two low lying excited singlet states with available experimental data. Two-photon spectroscopy was used to measure the vibrational frequencies of these symmetry species in the S_1 and S_2 state in low-temperature *n*-heptane,[26] biphenyl,[27] and argon[1] matrices. We shall mostly use the more recent argon matrix results, in which a better resolution and signal to background ratio were obtained.

As summarized in Table 3, the calculated vibrational frequencies of the b_{1u} modes of S_1 agree pretty well with the observed frequencies. The assignment of the low-frequency ν_{11}, ν_{10}, and ν_9 modes agrees with that of ref 1. The 1212 cm^- band has been tentatively assigned to the $\nu_s(b_{1u})$ mode by WH, but according to the calculation, it is better described as the $\nu_7(b_{1u})$ mode. The observed 1281 cm^{-1} feature is probably due to the $\nu_6(b_{1u})$ fundamental (calc 1288 cm^{-1}), rather than the proposed[1] $\nu_7(b_{1u}) + \nu_{12}(a_u)$ combination. The weak band at 1469 cm^{-1} is close in energy to the calculated $\nu_s(b_{1u})$ at 1431 cm^{-1}, and the stronger 1531 cm^{-1} one is assigned as the $\nu_4(b_{1u})$ mode (calc 1528 cm^{-1}). The weak unassigned 1425 and 1559 cm^{-1} bands are probably part of the $S_0 \rightarrow S_2$ spectrum, as discussed below.

The origin of the $S_0 \rightarrow S_2$ transition is calculated to lie 0.62 eV higher than that of $S_0 \rightarrow S_1$ and to have an oscillator strength of 0.0006, much smaller than the calculated S_1 value, $f = 0.23$. These results are in qualitative agreement with experiment and predict that the $S_0 \rightarrow S_2$ transition is likely to be masked by the more intense $S_0 \rightarrow S_1$ one. The experimental estimate for the energy gap between the two states in the gas phase is smaller, about 0.05 eV.[1] The assignments proposed in ref 1 for the vibrational levels of this state are largely confirmed by the calculation. Only some a_g and b_{2u} modes are experimentally observed with certainty. The calculated values for the three a_g modes are in very good agreement with experiment. The expectation that the "Kekulé-type" b_{2u} modes will be the most prominent in the $1^1A_g \rightarrow 1^1B_{2u}$ spectrum is substantiated by this work. However, a certain change in the assignments and the level order is called for by the calculation, as discussed in section IV.c.

III.b.2. The Triplet $^3B_{1u}$ State. Vibrational frequencies in the triplet state of anthracene were studied by infrared[28] and Raman[29,30] spectroscopies. The frequencies of several strong transitions have been firmly established, but in view of technical difficulties, the uncertainty in the determination of many weaker bands is large. Table 4 summarizes the observed strong bands and their suggested assignments by the authors of refs 28 and 30. Table 4 also lists assignments based on the results listed in Table 3, taking into account the calculated frequencies as well as the IR and Raman intensities. Raman intensities for the triplet state were not calculated, and the values given in Table 4 were calculated for the ground state at the HF level using the 3-21G basis set. The calculated frequencies of most observed lines are seen to agree fairly well with the experimental values.

In most cases, the proposed mode descriptions in the original papers are supported by the calculation, but some differences

TABLE 3: Vibrational Frequencies of the S_0, S_1, S_2, and T_1 States of Anthracene, Using the 3-21G Basis Set[a]

mode	number	S_0 calc	S_0 exptl[b]	S_1 calc	S_1 exptl[c,d]	S_2 calc	S_2 exptl[d]	T_1 calc	T_1 exptl	mode	number	S_0 calc	S_0 exptl[b]	S_1 calc	S_1 exptl[c,d]	S_2 calc	S_2 exptl[d]	T_1 calc	T_1 exptl
										In-Plane									
a_g	12	383	397	380	389	384		372		b_{1u}	11	229	234	229	214	230		230	
	11	636	625	610	587	620		616			10	640	653	657	640	631		665	
	10	733	754	707	728	680	712	718			9	908	906	896	891	897		886	
	9	955	1007	996	1025	967	1020	971			8	1156	1147	1096	1029(?)	1132		1080	
	8	1182	1164	1165	1140	1174		1097			7	1257	1272	1227	1212	1239		1191	
	7	1214	1264	1207	1184	1243		1156	1158[e]		6	1300	1317	1288	1282	1285		1282	1282[e]
	6	1366	1412	1280	1387	1313	1413	1229	1365[e]		5	1435	1448	1431	1469	1436		1428	1434[g]
	5	1455	1480	1460	1504	1467		1448	1459[e]		4	1620	1620	1528	1513	1551		1484	
	4	1541	1556	1515	1595	1494		1516	1564[e]		3	2974	3007	2976		2975		2978	
	3	2976	3027	2974		2977		2987			2	2979	3053	2983		2982		2987	
	2	2984	3048	2987		2984		2990			1	2997	3084	2999		3001		2997	
	1	3011	3062	3015		3017		3012		b_{2u}	11	605	601	601	590	606	593[h]	606	
b_{3g}	11	392	397	378	390$_{(g)}$[f]	384		381			10	756	809(?)	772	806(?)	735	727[h]	770	
	10	531	521	519	498	523		528			9	940	998	994		960	969[h]	905	
	9	914	903	897	877	903		893			8	1044	1124[i]	1102		1140	1110[h]	1017	
	8	1074	1102	1051	1045	1072		1044			7	1156	1162	1129		1169	1165[h]	1112	
	7	1193	1187	1151	1170	1196		1160	1182[e]		6	1269	1346	1187		1601	1548[h]	1179	
	6	1281	1273	1252	1291	1261		1231			5	1364	1397	1300		1265		1306	
	5	1391	1433	1387	1325	1390		1380			4	1443	1495	1443		1440	1449[h]	1446	1450[g]
	4	1571	1574	1405	1476	1512		1415			3	1521	1534	1508		1467	1479[h]	1497	
	3	1620	1627	1473	1530	1620		1458			2	2982	3021	2985		2983		2984	
	2	2978	3005	2981		2981		2980			1	3010	3048	3014		3016		3012	
	1	2997	3054	2999		3001		2997											
										Out-of-Plane									
b_{1g}	4	220	242	231		218		225		a_u	5	116	137	79		87		116	
	3	463	477	421		420		426			4	479	552	494		439		498	
	2	746	747	712		704		722			3	733	743	683		668		700	
	1	974	956	909		925		908			2	845	858	842		813		844	
b_{2g}	6	254	284	230	232[f]	198		237			1	1001	958	965		950		970	
	5	564	577	513	541[f]	484		529		b_{3u}	6	86	96	77		80		74	
	4	760	771	690		686		678			5	365	383	322		332		318	
	3	824	896	769	748[f]	780		762			4	456	504	390		397		412	
	2	923	916	891	905[f]	866		864			3	718	732	701		690		700	719[e]
	1	1003	975	961	967[f]	953		972			2	899	892	833		840		764	779[e]
	1	980	952	918		933		909	899[e]										

[a] In-plane calculated frequencies listed are scaled by 0.89; out-of-plane ones, by 0.85. Question marks next to experimental values indicate uncertain assignments. [b] Experimental data from ref 42. [c] Argon matrix experimental data from refs 1 and 2. [d] Argon matrix experimental data from ref 1. [e] Benzene solution experimental data from ref 30. [f] Gas phase value from ref 39 (matrix value not available). [g] Nitrogen matrix experimental data from ref 28. [h] For the level ordering of the b_{2u} vibronic states in the $^1B_{2u}$ state, see Figure 4. [i] 1068 cm^{-1} according to ref 37 (anthracene crystal).

TABLE 4: Assignment of the Observed Vibrational Frequencies of the $^3B_{1u}$ State

experimental frequency	method[a]	assignment[b]	ref	theory frequency	intensity[c]		assignment
384	R	a_g(vw)	41	372	18	a_g	skel. deform
604	R	a_g(vw)	41	616	1.3	a_g	skel. deform
740	R	a_g(vw)	41	718	43	a_g	skel. deform
719	IR	CH oop bend	28	734	57	$3b_{3u}$	CH oop bend
779[d]	IR		28	800	167	$2b_{3u}$	CH oop bend
886	IR	CH oop bend	28	862	30[e]	$4b_{3u} + 2b_{1g}$	skel. deform
899	IR	skel. deform	28	952	13	$1b_{3u}$	skel. deform
1026	R	a_g(w)	41	971	27	a_g	CH ip bend
1158	R	a_g	30, 41	1156	182	$7a_g$	CH ip bend
1182	R	a_g(m)	29, 30, 41	1160	65	$7b_{3g}$	CH ip bend
1282	IR	CH ip bend	28	1282	4	$6b_{1u}$	CH ip bend
1365[f]	R	a_g	29, 30, 41	1229	758	$6a_g$	skel. deform
1434	IR	CC ring str.	28	1428	18	$5b_{1u}$	CH ip bend
1450	IR	CC ring str.	28	1446	25	$4b_{2u}$	CH ip bend
1459	R	a_g(m)	29, 30, 41	1448	73	$5a_g$	skel. deform
1564	R	a_g(w)	29, 30, 41	1516	149	$4a_g$	skel. deform

[a] IR, infrared; R, Raman. [b] The assignments as proposed in the cited papers. [c] Calculated IR intensity in km/mol; Raman scattering intensities (Å^4/amu) were calculated for the corresponding ground state vibrations at the HF/3-21G level. [d] The most intense observed IR band. [e] This is the calculated IR intensity of the $4b_{3u}$ fundamental (calc frequency, 431 cm^{-1}). [f] The most intense observed Raman band.

should be noted. The two high-frequency Raman bands at 1564 and 1459 cm^{-1} are essentially symmetric skeletal deformations of the carbon atoms. The two high-frequency IR bands at 1450 and 1434 cm^{-1} are calculated as primarily CH in-plane bending motions, rather than CC ring stretch, although this latter motion is also involved in the mode. The IR band at 1282 cm^{-1} is calculated to have a rather weak intensity, but except for the proposed one, there is no calculated band in the relevant energy range with a higher IR intensity. The possibility that this band is actually due to a combination band cannot be ruled out at

this point. One possibility is the $\nu_2(b_{2u}) + \nu_{11}(a_g)$ combination. The $\nu_2(b_{2u})$ mode is calculated to have an IR intensity of 8.7 km/mol and a 667 cm^{-1} frequency. Using the experimental value[30] for the $\nu_{11}(a_g)$ mode (600 cm^{-1}), the combination is calculated to be 15 cm^{-1} to the red of the observed band.

The 899 cm^{-1} is assigned as the $\nu_1(b_{3u})$ mode, calculated at 952 cm^{-1} and having a reasonable IR intensity (see Table 4). However, the nearby 886 cm^{-1} band has no obvious assignment for any fundamental. The strongly IR active $\nu_4(b_{3u})$ mode (calculated frequency 412 cm^{-1}, IR intensity 30 km/mol) was outside the spectral range of the measurement (550−1650 cm^{-1}) and thus could not be observed separately. The 886 cm^{-1} feature could be due to the $\nu_4(b_{3u}) + \nu_3(b_{1g})$ combination transition, ($b_{3u} \times b_{1g} = b_{2u}$, making it, in principle, IR active).

IV. Discussion

IV.a. Comparison of the CIS with the UHF Calculations. The basic conclusions of the former study that used the UHF method[2] are confirmed in this work. In particular, the lengthening of the C1−C2 and C9−C11 bonds and the shortening of the C2−C3 and C1−C11 bonds in both S_1 and S_2 are a result of a transfer of an electron from the two highest occupied molecular orbitals to the two lowest unoccupied ones (Scheme 1).

The energies of the excited singlet states are calculated to be higher than the experimental values. In particular the S_1-S_2 separation is calculated to be 0.62 eV, while the most recent experimental value is 0.1 eV.[1] This may result from the neglect of the contribution of double, triple, and higher multiple excitation configurations. Partial correction for this effect can be achieved by applying second-order Moller−Plesset perturbation treatment. Indeed, the S_1-S_2 gap is calculated at the CIS-MP2 level to be only 0.15 eV.

The vibrational frequencies of the first excited state ($^1B_{1u}$ in the Mulliken convention used in this paper, $^1B_{2u}$ in the Pariser convention used in ref 2) are similar to those calculated by the UHF method. The present calculation differs from the previous one only in a few cases. A rather large mismatch was noted between the calculated two lowest frequency b_{3g} modes and the experimental jet values (ref 39) of 390 and 473 cm^{-1}. The CIS results, 378 and 519 cm^{-1}, respectively, are in much better agreement with experiment than the UHF ones (447 and 574 cm^{-1}).

Since the main purpose of the present calculation was the assignment of the vibronic structure of the electronic transitions from the ground state, it is appropriate to consider the reliability of the method. The CIS method was criticized as being inadequate in some cases since it neglects the contribution of doubly (and higher) excited configurations.[31] Since large-scale computations are often impractical for molecules the size of anthracene, it has been proposed that other configuration interaction methods, such as the complete active space (CAS) one,[32] offer a better approximation. In the practical implementation of these, one chooses several reasonable configurations and tests their suitability for the problem at hand. For electronically excited states of molecules such as benzene, a calculation with 12 active π orbitals leads to a large error, which may be remedied by applying second-order perturbation treatment.[31] A calculation of the normal modes was not given. For molecules the size of anthracene, the CIS calculation is practical and appears to provide an adequate zeroth-order treatment for the excited states discussed in this paper. Other methods are either very expensive computationally or necessarily restrictive in the number of configurations used. Their suitability for assigning the vibronic structure of electronically excited states still needs to be tested. On the other hand, the good match of the CIS frequencies to the experimental values seems not to be accidental in view of past results.[2,33,34]

SCHEME 2: Diagram Showing Valence Bond Kekulé-Type Structures of Benzene and the Symmetry-Adapted Vibrational Mode That Couples Them

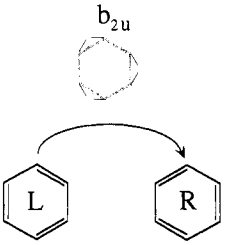

SCHEME 3: Diagram Showing Valence Bond Kekulé-Type Structures of Anthracene and the Symmetry-Adapted Vibrational Modes That Couple Them (The Upper Part Shows Two Structures in Which the Double Bonds Alternate in the Central Ring; the Lower Part, Structures in Which Double-Bond Alternation Extends over the Whole Periphery of the Molecule)

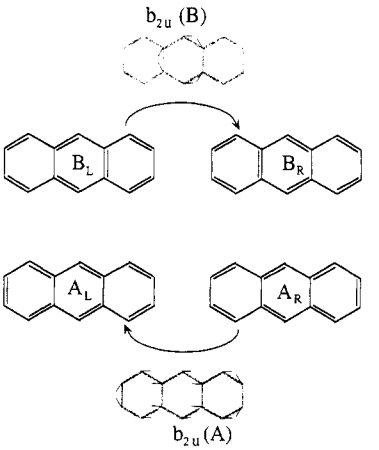

IV.b. A Simplified Valence Bond Description of the Electronic States of Anthracene. In this section we review briefly the valence bond description of the electronic states of anthracene, with a special emphasis on the 1^1B_{2u} state. A more complete treatment is given in a forthcoming paper.[35] The main contribution to the total wave function of the ground state and the lowest lying $^1B_{2u}$ state of benzene comes from the two Kekulé-type structures[10,18] (see Scheme 2). Denoting the structures as L and R and their corresponding wave functions as $\Psi(L)$ and $\Psi(R)$, respectively, the wave functions for $S_0(1^1A_g)$ and $S_2(1^1B_{2u})$ may be written approximately as

$$\Psi(S_0(^1A_g)) = 2^{-1/2}(\Psi(L) + \Psi(R)) \quad (1a)$$

$$\Psi(S_1(^1B_{2u})) = 2^{-1/2}(\Psi(L) - \Psi(R)) \quad (1b)$$

The four Kekulé structures of anthracene are shown in Scheme 3; it is seen that the two upper structures are benzenic types, involving π-bond shift in the central ring only. As such, these structures will be denoted as B_L and B_R; their corresponding wave functions as $\Psi(B_L)$ and $\Psi(B_R)$, respectively. In the lower pair, π-bond shift is annulenic and extends over the periphery of the molecule; these structures will be refered to as A_L and A_R; their corresponding wave functions, as $\Psi(A_L)$ and $\Psi(A_R)$, respectively. By analogy with benzene, and on the basis of symmetry considerations, the in-phase combination of the four Kekulé structures will contribute significantly to the ground

state description:

$$\Psi(S_0(^1A_g)) = c_B\{\Psi(B_L) + \Psi(B_R)\} + c_A\{\Psi(A_L) + \Psi(A_R)\} \quad (2a)$$

Similarly, the wave function of the lowest lying $^1B_{2u}$ state in anthracene (which is S_2) may be written as the linear combination of out-of-phase combinations which possess the proper B_{2u} symmetry:

$$\Psi(S_2(^1B_{2u})) = c_B^*\{\Psi(B_L) - \Psi(B_R)\} + c_A^*\{\Psi(A_L) - \Psi(A_R)\} \quad (2b)$$

Scheme 2 shows that structures L and R are interconverted by a Kekulé-type vibrational motion; among the normal mode of benzene, the $\nu_{14}(b_{2u})$ mode is the most similar to this motion. Indeed, it is the $\nu_{14}(b_{2u})$ mode that was found to undergo the large frequency increase upon $1^1A_g \rightarrow 1^1B_{2u}$ excitation. This result can be rationalized by considering the avoided crossing model,[10] using the VB states, eqs 1a and 1b.[36] By analogy, one is prompted to look for normal modes of anthracene that have symmetry similar to the modes that interchange the Kekulé structures of anthracene (shown in Scheme 3). As seen from the scheme, the B_R and B_L structures undergo an interchange (and thus avoided crossing) along a b_{2u} mode that moves the central ring's carbon atoms in an alternating manner. The A_R and A_L structures are interconverted by another b_{2u}-type mode that moves the carbon atoms on the periphery in an alternating manner, and it is along the symmetry coordinates of these two modes that avoided crossing between the respective structures will take place. It follows that the $S_0(1^1A_g)$ (eq 2a) and the $S_2(1^1B_{2u})$ (eq 2b) states are mutually related by avoided crossings along two specific b_{2u} coordinates, and by analogy to the situation in benzene, it is expected that *two* such modes will undergo a frequency up-shift upon transition from the S_0-(1^1A_g) to the $S_2(1^1B_{2u})$ state.

As an aside, one notices that no b_{2u} mode can interchange structures A_L and B_L, or A_R and B_R. Thus, consideration of all b_{2u} modes shows that the avoided crossing model predicts that *only* two modes are expected to exhibit the frequency increase.

IV.c. Correlation of the CIS-Calculated b_{2u} Modes with the Symmetry-Adapted Modes That Interchange VB Kekulé Structures. The calculation of normal mode frequencies and displacements by the VB method is impractical, while the MO-CIS calculation readily provides information on normal modes, in which both carbon and hydrogen atoms participate. Inspection of the atomic displacement vectors of the calculated modes allows one to correlate them with the symmetry-adapted modes which interconnect the VB structures shown in Scheme 3. Thus, the $\nu_6(b_{2u})$ mode is related to the symmetry mode connecting structures B_L and B_R. Figure 2 shows the vector displacements calculated for this mode in the S_0 and S_2 states, revealing that in both states a Kekulé-type motion is taking place primarily in the central ring. In the ground state, both carbon and hydrogen atoms participate in the motion. In the S_2 state, the amplitude of the carbon atom motion is greatly increased, at the expense of the hydrogens, accounting for the large increase in the reduced mass of the mode. The (scaled) frequency in the ground state is calculated to be 1269 cm^{-1}; in the B_{2u} state, 1601 cm^{-1}. Experimentally, the corresponding frequencies are 1346 and 1548 cm^{-1}, respectively. It is concluded that experiment supports the theoretical analysis and VB predictions, although the magnitude of the effect is smaller than the CIS-calculated values. Figure 2 also shows the $5b_{2u}$ mode of the ground state (calculated frequency 1364 cm^{-1}) and the corresponding mode in S_2 (calculated frequency 1265 cm^{-1}). It is

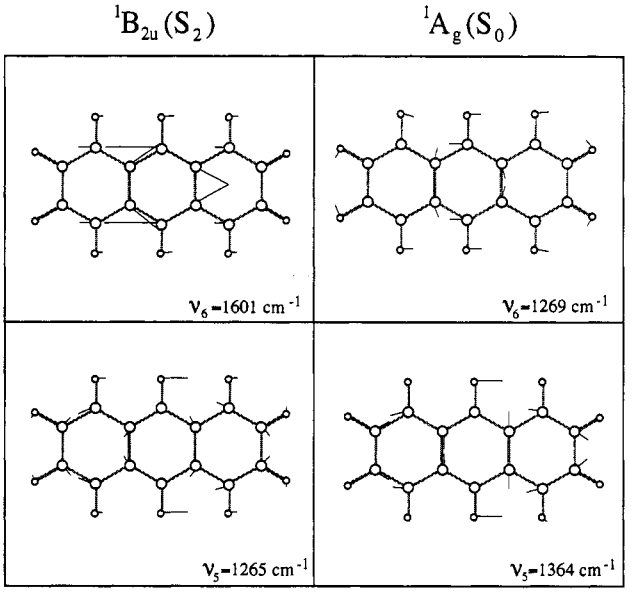

Figure 2. Vector displacement diagrams for the ν_5 and ν_6 b_{2u} vibrations of anthracene. The "inner" ring ν_6 mode undergoes a considerable frequency increase upon electronic excitation (from calc 1269, exptl 1346 cm^{-1} in S_0 to calc 1601, exptl 1548 cm^{-1} in S_1), while the "outer" ring ν_6 mode undergoes a small frequency decrease.

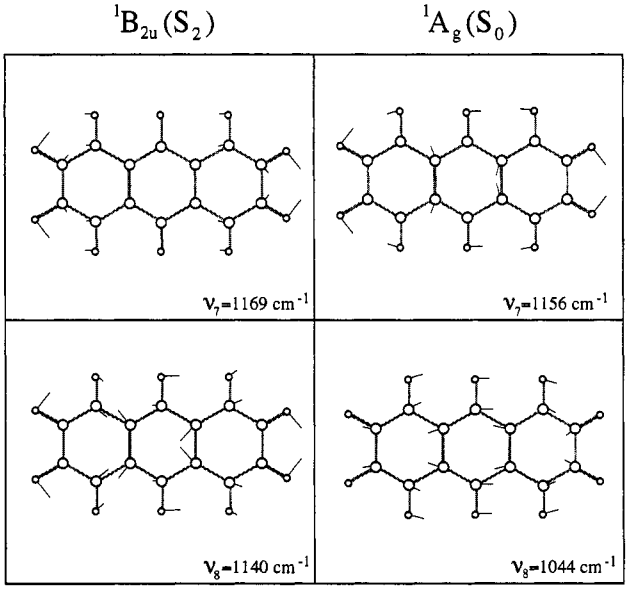

Figure 3. Vector displacement diagrams for the ν_7 and ν_8 b_{2u} vibrations of anthracene. The annular ν_8 mode is calculated to undergo a frequency increase upon electronic excitation (from 1044 cm^{-1} in S_0 to 1140 cm^{-1} in S_1). See text for comparison with experiment.

seen that in this case the Kekulé-type motion is centered on the outer rings of the molecule, and the motion becomes more hydrogen-like in the excited state. In this case the usual frequency decrease expected upon electronic excitation is observed.

The model predicts another symmetry-adapted mode whose frequency should increase, the one that interconverts structures A_L and A_R of Scheme 3. Figure 3 shows two other b_{2u} modes, ν_7 and ν_8. The latter is mainly an annulene mode, in which the motion of the carbon atoms is along the periphery of the molecule and its atom displacements are similar to those of the mode shown below structures A_L and A_R in Scheme 3. A frequency increase is indeed calculated for this mode upon excitation to the B_{2u} state, albeit much smaller than in the case of ν_6, from 1044 to 1140 cm^{-1}. Figure 4 shows a correlation diagram connecting the calculated b_{2u} modes of the molecule

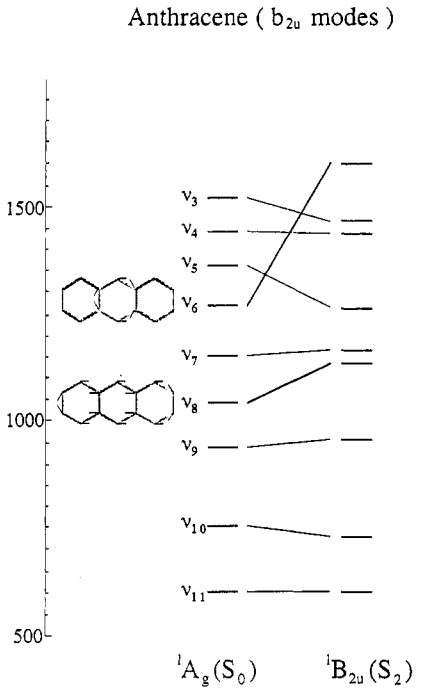

Figure 4. Correlation diagram showing the correlation between b_{2u} vibrational modes in S_0 and in S_2. The motion in the ν_6 and ν_8 b_{2u} modes is emphasized by the shaded areas and illustrated by the lines emanating from the carbon atoms.

TABLE 5: Assignment of the Vibrational Frequencies of the $^1B_{2u}$ State That Were Observed by Two-Photon Fluorescence Excitation Spectroscopy

experimental[a]			theory	
energy (cm^{-1})	intensity[b]	assignment[c]	energy (cm^{-1})	assignment
593	1	n.p.	601	$11b_{2u}$
820	8	$3b_{2u}$ or $4b_{1u}$ of S_1	735	$10b_{2u}$
969	22	$9b_{2u}$	960	$9b_{2u}$
1110	16	$4b_{1u} + 12a_g$ of S_1	1140	$8b_{2u}$
1165	72	$7b_{2u}$	1169	$7b_{2u}$
1449	54	$6b_{2u}$	1440	$4b_{2u}$
1479	81	$5b_{2u}$	1467	$3b_{2u}$
1548	100	$4b_{2u}$	1601	$6b_{2u}$

[a] In an argon matrix,[1] energy with respect to the origin of the band assumed for site III at 28 000 cm^{-1}. [b] Relative intensity in arbitrary units. [c] As proposed in ref 1; n.p., not proposed.

in S_0 with those of S_2. It is seen that an increase in frequency is found only for the benzenic ν_6 and the annulenic ν_8 modes.

Comparison with experiment for the $\nu_8(b_{2u})$ mode is more difficult than for the $\nu_6(b_{2u})$ mode (Table 5). Wolf and Hohlneicher[1] refrain from assigning an experimental value for the $\nu_8(b_{2u})$ mode of the B_{2u} state, placing it somewhere between 969 (their suggestion for the $\nu_9(b_{2u})$ mode's frequency) and 1165 cm^{-1} (their proposed $\nu_7(b_{2u})$ mode's frequency). We suggest that the weak band observed at 1942 cm^{-1} above the origin of the $^1B_{1u}$ state (Table 2 in ref 1, assigned tentatively to a combination band in $^1B_{1u}$) may be due to this mode (cf. Table 3). Even the assignment of the ground state value is controversial, proposed values varying between 1068[37] and 1124[38] cm^{-1}. A recent IR study of anthracene in an argon matrix[11] failed to report a value for this mode's frequency. Thus, the experimental validation of the arguments proposed by the calculation remains at present uncertain. Our assignments are listed in Table 5, which also reproduces WH's proposed assignments. The frequency increase calculated for this mode is much smaller than for the ν_6 mode; the calculation was done in the harmonic approximation, neglecting possible anharmonic interactions, Fermi resonances, and other interactions. The apparent small experimental frequency change may reflect the importance of these interactions. The stronger effect observed for the "inner" Kekulé-type vibration ν_6 makes it better suited for comparison with theoretical considerations.

The relationship between the vibrational modes and the interconversion of the VB structures offers a simple experimental criterion for studying the electronic structures of large molecules. The case of the b_{2u} modes of small aromatic molecules is particularly revealing, since the frequency exaltation upon electronic excitation is so dramatic. Unfortunately, experimental measurement of the frequency of these modes in the B_{2u} state is possible only by two-photon absorption, making it a hard-to-get quantity. Nevertheless, the investigation of electronically excited states appears to offer important insight into the electronic structure of the *ground* state and is thus of interest to the general chemical community.

V. Conclusions

The MO-CIS method is found to be useful for predicting the properties of the low lying electronic states of anthracene. Good agreement between the calculated structure, vibrational frequencies and transition probabilities, and experimental values is obtained. Most vibrational frequencies are found to decrease upon electronic excitation; the fairly large *increased* frequency of the $\nu_6(b_{2u})$ mode in the $S_2(1^1B_{2u})$ state as compared with the $S_0(1^1A_g)$ ground state is accounted for in the VB picture, using the Kekulé-type wave functions as the main structures contributing to the total wave functions of S_0 and S_2. VB theory cannot be used for a direct computation of vibrational frequencies of electronically excited states of medium sized molecules, but its combination with an MO-based calculation is shown to be useful for providing a lucid physical interpretation of the data.

Acknowledgment. We thank Dr. R. Fraenkel for many enlightening discussions. The Farkas Center for light−matter interaction is supported by the Minerva Gesellschaft mbH, Munich. S.S. thanks the ISF for partial support of this project.

References and Notes

(1) Wolf, J.; Hohlneicher, G. *Chem. Phys.* **1994**, *181*, 185.
(2) Zilberg, S.; Samuni, U.; Fraenkel, R.; Haas, Y. *Chem. Phys.* **1994**, *186*, 303.
(3) Platt, J. R. *J. Chem. Phys.* **1949**, *17*, 484.
(4) In this work we use Mulliken's convention (Mulliken, R. S. *J. Chem. Phys.* **1955**, *231*, 1997) in which the x axis is perpendicular to the molecular plane and the y axis lies along the long in-plane axis, leading to $x = B_{3u}$, $y = B_{2u}$, and $z = B_{1u}$. The $S_0 \rightarrow S_1$ transition is thus a $1^1A_g \rightarrow 1^1B_{1u}$ one, and the $S_0 \rightarrow S_2$ is $1^1A_g \rightarrow 1^1B_{2u}$. In the previous paper, Pariser's convention was used, in which the $S_0 \rightarrow S_1$ transition is designated as $1^1A_g \rightarrow 1^1B_{2u}$. The Mulliken convention was chosen since it is the most commonly used one in the discussion of Kekulé forms of benzene and its derivatives. In it, the D_{3h} distortive vibration transforms as b_{2u}.
(5) Callis, P. R.; Scott, T. W.; Albrecht, A. C. *J. Chem. Phys.* **1983**, *78*, 16.
(6) Wunsch, L.; Metz, F.; Neusser, H. J.; Schlag, E. W. *J. Chem. Phys.* **1976**, *66*, 386.
(7) Friedrich, D. M.; McClain, W. M. *Chem. Phys. Lett.* **1975**, *32*, 541.
(8) Mikami, N.; Ito, M. *Chem. Phys.* **1977**, *23*, 141.
(9) Haas, Y.; Zilberg, S. *J. Am. Chem. Soc.* **1995**, *117*, 5387.
(10) Shaik, S. S.; Hiberty, P. C.; Ohanessian, G.; Lefour, J.-M. *J. Phys. Chem.* **1988**, *92*, 5086, and references therein.
(11) Sczepanski, J.; Vala, M.; Talbi, D.; Parisel, O.; Ellinger, Y. *J. Chem. Phys.* **1993**, *98*, 4494.
(12) Zerbetto, F.; Zgierski, M. Z. *J. Chem. Phys.* **1993**, *98*, 4822. Orlandi, G.; Palmieri, P.; Tarroni, R.; Zerbetto, F.; Zgierski, M. Z. *J. Chem. Phys.* **1994**, *100*, 2458.
(13) Walters, V. A.; Hadad, C. M.; Thiele, Y.; Colson, S. D.; Wiberg, K. B.; Johnson, P. M.; Foresman, J. B. *J. Am. Chem. Soc.* **1991**, *113*, 4782. Wiberg, K. B.; Hadad, C. M.; Foresman, J. B.; Chupka, W. A. *J. Phys. Chem.* **1992**, *96*, 10756.

(14) Swiderek, P.; Hohlneicher, G.; Maluendes, S. A.; Dupuis, M. *J. Chem. Phys.* **1993**, *98*, 974.
(15) Hehre, W. H.; Radom, L.; Schleyer, P. v. R.; Pople, J. A. *Ab-Initio Molecular Orbital Theory*; Wiley: New York, 1986.
(16) Foresman, J. B.; Head-Gordon, M.; Pople, J. A.; Frisch, M. J. *J. Chem. Phys.* **1992**, *96*, 135.
(17) Shaik, S. In *New Theoretical Concepts for Understanding Organic Reactions*; Bertran, J.; Csizmadia, I. G., Eds.; NATO, ASI Series, Kluwer: Dordrecht, 1989; Vol. 267, p 165.
(18) da Silva, E. C.; Gerratt, J.; Cooper, D. L.; Raimondi, M. *J. Chem. Phys.* **1994**, *101*, 3866.
(19) Frisch, M. J.; Trucks, G. W.; Head-Gordon, M.; Gill, P. M. W.; Wong, M. W.; Foresman, J. B.; Johnson, B. G.; Schlegel, H. B.; Robb, M. A.; Replogle, E. S.; Gomperts, R.; Andres, J. L.; Raghavachari, K.; Binkley, J. S.; Gonzalez, C.; Martin, R. L.; Fox, D. J.; Defrees, D. J.; Baker, J.; Stewart, J. J. P.; Pople, J. A. *Gaussian 92*, Revision F2; Gaussian: Pittsburgh, PA, 1992.
(20) Suzuki, H. *Electronic Absorption Spectra and Geometry of Organic Molecules*; Academic Press: New York, 1967; p 117.
(21) Hehre, W. J.; Ditchfield, R.; Pople, J. A. *J. Chem. Phys.* **1972**, *56*, 2257.
(22) Pople, J. A.; Scott, A. P.; Wong, M. W.; Radom, L. *Isr. J. Chem.* **1993**, *33*, 345.
(23) Pariser, R. *J. Chem. Phys.* **1956**, *24*, 250.
(24) Baskin, J. S.; Zewail, A. H. *J. Phys. Chem.* **1989**, *93*, 5701, Table 1.
(25) Fraenkel, R.; Samuni, U.; Haas, Y.; Dick, B. *Chem. Phys. Lett.* **1993**, *203*, 523.
(26) Salvi, P. R.; Marconi, G. *J. Chem. Phys.* **1986**, *84*, 2542.
(27) Bree, A.; Leyderman, A.; Taliani, C. *Chem. Phys. Lett.* **1985**, *118*, 468.
(28) Hoesterey, B.; Mitchell, M. B.; Guillory, W. L. *Chem. Phys. Lett.* **1987**, *142*, 261.
(29) Beck, S. M.; Brus, L. E. *J. Chem. Phys.* **1981**, *75*, 1031.
(30) van Zeyl, P. H. M.; Varma, C. A. G. O.; Vroege, G. *Chem. Phys. Lett.* **1984**, *105*, 127.
(31) Roos, B. O.; Andersson, K.; Fülscher, M. P. *Chem. Phys. Lett.* **1992**, *192*, 5.
(32) Roos, B. O.; Taylor, P. R.; Siegbahn, P. E. M. *Chem. Phys.* **1980**, *48*, 157.
(33) Zilberg, S.; Haas, Y. *J. Chem. Phys.* **1995**, *103*, 20.
(34) Kendler, S.; Zilberg, S.; Haas, Y. *Chem. Phys. Lett.* **1995**, *242*, 139.
(35) Shaik, S.; Zilberg, S.; Haas, Y. In preparation.
(36) Shaik, S.; Shurki, A. In preparation.
(37) Bree, A.; Kydd, R. A. *J. Chem. Phys.* **1968**, *48*, 5319.
(38) Bakke, A.; Cyvin, B. N.; Whitmer, J. C.; Cyvin, S. J.; Gustavsen, J. E.; Klaeboe, P. *Z. Naturforsch.* **1979**, *34a*, 579.
(39) Lambert, W. R.; Felker, P. M.; Syage, J. A.; Zewail, A. H. *J. Chem. Phys.* **1984**, *81*, 2195. Lambert, W. R.; Felker, P. M.; Zewail, A. H. *J. Chem. Phys.* **1984**, *81*, 2209. Peng, L. W.; Keelan, B. W.; Semmes, D. H.; Zewail, A. H. *J. Phys. Chem.* **1988**, *92*, 5540.
(40) Ferguson, J.; Mau, A. W.-H. *Mol. Phys.* **1974**, *28*, 469.
(41) Tripathy, G. N. R.; Fisher, M. R. *Chem. Phys. Lett.* **1984**, *104*, 297.
(42) Räsänen, J.; Stenman, F.; Penttinen, E. *Spectrochim. Acta* **1973**, *29A*, 395. Cyvin, B. N.; Cyvin, S. J. *J. Phys. Chem.* **1969**, *73*, 1430. Bakke, A. V.; Cyvin, B. N.; Whitmer, J. C.; Cyvin, S. J.; Gustavsen, J. E.; Klaeboe, P. *Z. Naturforsch.* **1979**, *34a*, 579. Evans, D. J.; Scully, D. B. *Spectrochim. Acta* **1964**, *20*, 891.

JP951522H